JOURNAL OF MATERIALS SCIENCE **34** (1999) 4097–4104

Modelling fracture in an Al_2O_3 particle reinforced AA 6061 alloy using Weibull statistics

K. M. MUSSERT, M. JANSSEN, A. BAKKER, S. VAN DER ZWAAG
Delft University of Technology, Department of Materials Science, Rotterdamseweg 137, 2628 AL Delft, The Netherlands

Fracture in an AA 6061 based metal matrix composite (MMC) containing 20 vol % Al_2O_3 particles is modelled using an axisymmetrical finite element model and a statistical approach for calculating the strength of reinforcing ceramic particles via the Weibull model. Within this model, variables such as the volume fraction, particle size and matrix alloy properties can be varied. When modelling the fracture behaviour of one particle, it is assumed that the survival probability of the ceramic particle is governed by a Weibull distribution. Fracture statistics of the MMC is examined by plotting the survival probability of an Al_2O_3 particle vs. the macroscopic axial stress applied on the whole MMC. Based on initial calculations it can be concluded that the relation between the macroscopic applied stress on the MMC and the survival probability of the ceramic particle can be described by the Weibull modulus m, as long as the stress distribution in the matrix surrounding the particle is proportional to the applied load and that triaxial loading of the MMC results in a lower survival probability compared to uniaxial loading. Fracture behaviour of MMCs can well be described and a 'mastercurve' can be made for various characteristic stresses and matrix yield stresses at a specific hardening exponent for the matrix material.

1. Introduction

Due to their high strength, high stiffness and high resistance to wear, ceramic particle reinforced metal matrix composites (MMCs) have attracted considerable attention in the past two decades. A reason for using any composite material is the extent to which the qualities of two or more constituents can be combined, without seriously accentuating their shortcomings [1]. The most widely applied metals as matrix material for MMCs are aluminium and its alloys, since their ductility, formability and low density can be combined with the stiffness and load-bearing capacity of the reinforcement. Microscopically, the mechanism of failure seems to depend on many factors, such as the strength of the interface between the particle and the surrounding matrix, the strength and reliability of the reinforcement and the matrix mechanical properties [2]. This paper describes an investigation into modelling of particle cracking.

To study the parameter dependence of Al_2O_3 particle fracture in a ductile AA 6061 aluminium matrix, an axisymmetrical finite element model based on a simple unit cell is used. A limitation of this continuum mechanics model is that there is no length scale included in the analyses and the results are thus insensitive to the microstructural size and specifically to the reinforcement size. However, this can be overcome by using Weibull statistics.

Work on commercial aluminium alloys reinforced with either Al_2O_3 or SiC particles [3–6] have demonstrated that reinforcements are broken progressively during plastic deformation and that the survival probability decreases with reinforcement size. In this paper, the survival probability of the reinforcing particles is assumed to be governed by a Weibull distribution. Within the cell model, variables such as, loading triaxiality, particle size, particle properties and matrix alloy properties are varied to investigate the parameter dependence of particle fracture.

2. Cell model

Micromechanical models for ductile damage and fracture are based on the notion that these physical processes can be described by the structural behaviour of relatively simple unit cells [7]. Cell model calculations are normally used to study microscopic voids in ductile materials [8]. However, in this research, a cell model is used to study metal matrix composites by simulating their behaviour for varying triaxiality of the stress state. An acceptable disadvantage of this approach is, that the relative position of the ceramic particles in the matrix is fixed.

The continuum is considered to consist of a periodic assemblage of hexagonal unit cells approximated by circular cylinders, see Fig. 1, which allows for an axisymmetrical calculation. Every cell of initial length $2L_0$ and radius R_0 contains a spherical particle of radius r_0. In order to simulate the constraint of the surrounding material, the cylindrical cell is required to remain cylindrical throughout the deformation history, i.e. the top

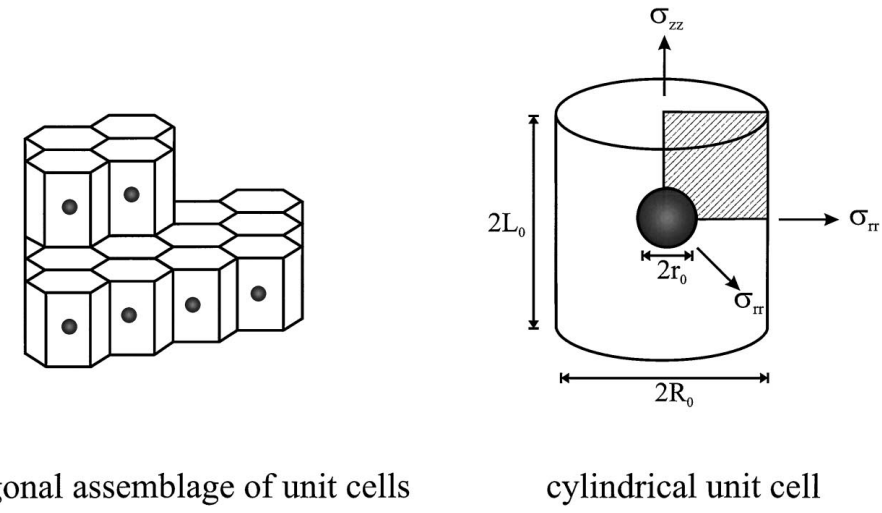

Figure 1 Micromechanical modelling of a matrix containing a spherical particle.

and bottom faces as well as both sides should remain flat and parallel.

During deformation, the surfaces normal to the axial and radial directions are subjected to homogeneous displacements in these directions respectively, whereby the ratio, ρ, of the average applied true stresses σ_{rr} and σ_{zz} is kept constant. This ratio is often called the stress proportionality factor and is given by [9]:

$$\rho = \frac{\sigma_{rr}}{\sigma_{zz}} \tag{1}$$

whereby σ_{rr} is the stress in the radial direction and σ_{zz} in the axial direction.

3. Weibull model

When modelling the survival probability of ceramic, the Weibull model [10] is often found to be applicable [11]. If one can assume the flaw size distribution to be fractal-like, this approach will be valid regardless of their size [12]. The size of a critical flaw will simply become smaller and the particle strength increases, as the particle volume decreases. A fractal distribution will ensure that there is always a distribution of flaws within the particles on a scale finer than the particle size.

Using Weibull statistics, the survival probability, S, of a ceramic particle volume, V, in case of a uniform stress distribution, is governed by

$$S = \exp\left\{-\frac{V}{V_0}\left(\frac{\sigma}{\sigma_0}\right)^m\right\} \tag{2}$$

where σ is the stress in the particle, σ_0 and V_0 are two constants with dimensions of stress and volume (σ_0 is often referred to as the characteristic stress), respectively, which are introduced for dimensional purposes [13] and m is the Weibull modulus. This equation can be rewritten, allowing a straight line representation of gradient m, when $\ln\ln(1/S)$ is plotted against $\ln\sigma$:

$$\ln\ln\frac{1}{S} = \ln\left(\frac{V}{V_0}\right) + m\cdot\ln\sigma - m\cdot\ln\sigma_0 \tag{3}$$

The strength of a ceramic particle is essentially limited by pre-existing critical flaws which are present in the material, i.e. surface and volume flaws. In the present model, it is assumed that flaws on the surface have no greater influence than those in the interior. If surface flaws dominate failure, then the volume term (V/V_0) should be replaced by an area term (A/A_0) [12].

4. Finite element calculations

The MMC is modelled with a matrix of AA 6061 (E = 69 GPa, $\nu = 0.33$, $\sigma_{ys} = 276$ MPa) and 20 vol % Al_2O_3 particles with a diameter of 4 or 8 μm ($E = 393$ GPa, $\nu = 0.27$, $\sigma_{ys} = 2000$ GPa, the latter is a fictitious high value to prevent plastic deformation in the ceramic particle). E is the Young's modulus, ν is Poisson's ratio and σ_{ys} is the yield stress. The behaviour of a ductile aluminium matrix is studied for two hardening exponent values n, (i.e. n = 4.35 and 14.94). The first is a value from literature for AA 6009-T4 [14] measured on tensile specimens in the extruded direction, the latter is a value measured in the laboratory, on tensile specimens AA 6061-T651 taken perpendicular to the extruded direction. The hardening exponent is defined in the uniaxial stress-strain relation in the form of a power law:

$$\varepsilon = \begin{cases} \dfrac{\sigma}{E} & \text{if } \varepsilon \le \dfrac{\sigma_{ys}}{E} \\ \dfrac{\sigma_{ys}}{E}\left(\dfrac{\sigma}{\sigma_{ys}}\right)^n & \text{if } \varepsilon > \dfrac{\sigma_{ys}}{E} \end{cases} \tag{4}$$

where E is the Young's modulus and σ_{ys} is the yield stress.

Finite element calculations were done for $\rho = 0$ (uniaxial tensile test) and 0.7 (triaxial tensile test). For all calculations, a particle with a diameter of 4 μm, m = 15, $\sigma_0 = 350$ MPa, $\sigma_{ys} = 276$ MPa, a hardening exponent for the matrix of $n = 14.94$ and $V_0 = 1$ mm^3 is considered to be the reference situation for the MMC.

In order to calculate the survival probability of a ceramic particle in an MMC, calculations on the cylindrical unit cell have been performed using the MARC finite element program [15]. The finite element mesh used for calculations consisted of 350 isoparametric quadrilateral 4-node elements (140 for the particle and 210 for the matrix), as shown in Fig. 2. Due to symmetry, only the region hatched in Fig. 1 needs to be considered.

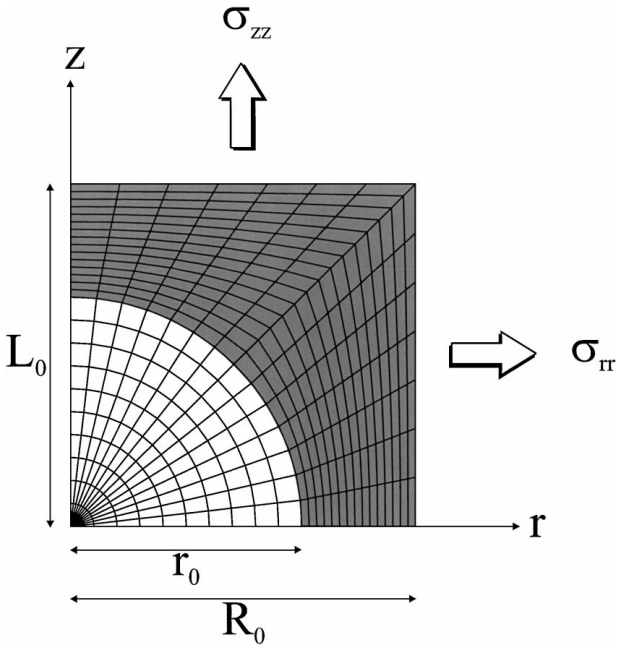

Figure 2 Finite element mesh used for calculations; z is axial direction and r is radial direction.

For every of the four integration points of each finite element belonging to the particle, the principal stresses σ_1, σ_2 and σ_3 are calculated and these values are averaged to get the three principal stresses for each element. Furthermore, the volume of each element is calculated. Using the stresses, the net applied stress σ in the particle is calculated using the Drücker-Prager criterion (from this point forward this stress will be denoted as σ_{DP}):

$$\sigma_{DP} = \sqrt{\tfrac{1}{2}\left[(\sigma_1-\sigma_2)^2+(\sigma_2-\sigma_3)^2+(\sigma_3-\sigma_1)^2\right]} + \tfrac{1}{3}\alpha(\sigma_1+\sigma_2+\sigma_3) \quad (5)$$

where α is related to the ratio of compression strength and tensile strength of the material and can be calculated using the following equation:

$$\alpha = 3\frac{(\sigma_c/\sigma_t - 1)}{(\sigma_c/\sigma_t + 1)} \quad (6)$$

where σ_c and σ_t are the compression strength and tensile strength respetively. In the present calculations $\sigma_c/\sigma_t = 10$ was used. Now, for a given σ_0 and m, the survival probability S can be calculated.

It should be mentioned that debonding of ceramic particles is excluded in this investigation, since the present model does not yet contain a criterion with which the occurrence of interface failure between the ceramic particle and its surrounding aluminium matrix can be calculated.

5. Results and discussion

In this investigation, the parameter dependence of particle fracture in proportional loading histories is examined. The parameters varied are the loading ratio via the constant ρ, the Weibull modulus m, the hardening exponent n for the matrix, the characteristic stress σ_0, the yield stress for the matrix σ_{ys} and the diameter of the ceramic particle. For all calculations, data are plotted against the macroscopic applied axial stress σ_{zz}, since σ_{DP} varies from element to element.

5.1. Reference configuration

In Fig. 3, the survival probability is plotted as a function of the macroscopic axial stress applied on the unit cell for the reference state of the MMC.

Regarding $\rho = 0.7$, this calculation results in a straight line of gradient 15 which is the value that was used for the Weibull modulus m. When comparing loading ratios $\rho = 0$ and 0.7, it can be seen that at lower stresses both calculations result in a straight line of

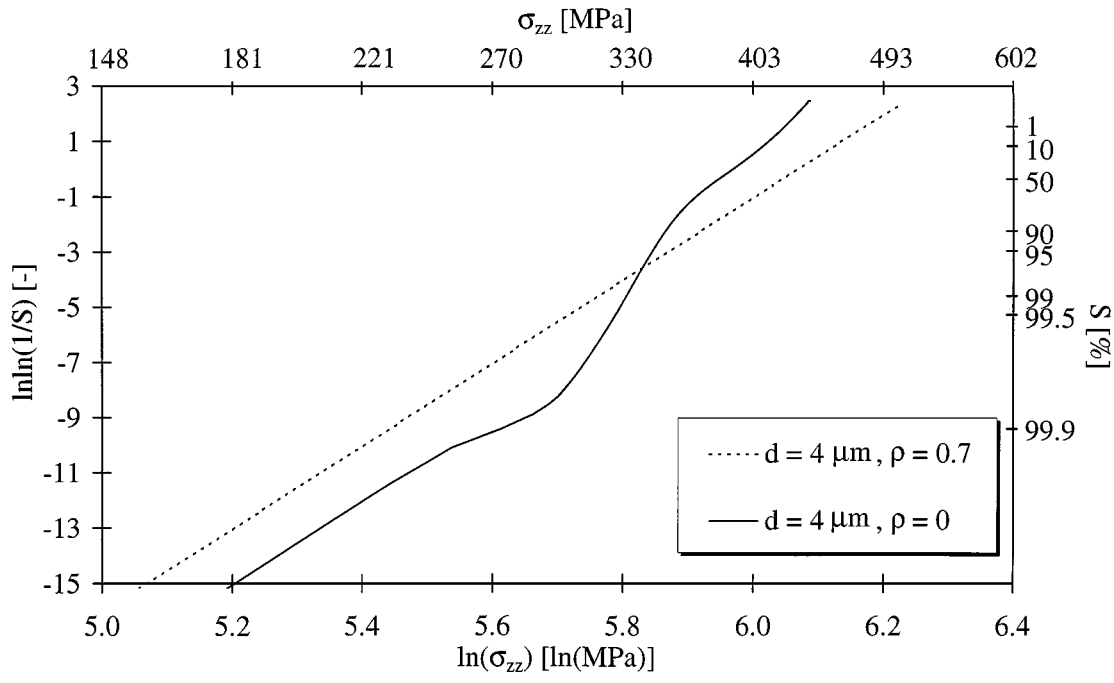

Figure 3 The survival probability S as a function of macroscopic axial stress σ_{zz} for a particle with a diameter of 4 μm with loading ratios $\rho = 0$ and 0.7 ($m = 15$, $\sigma_0 = 350$ MPa, $\sigma_{ys} = 276$ MPa and $n = 14.94$).

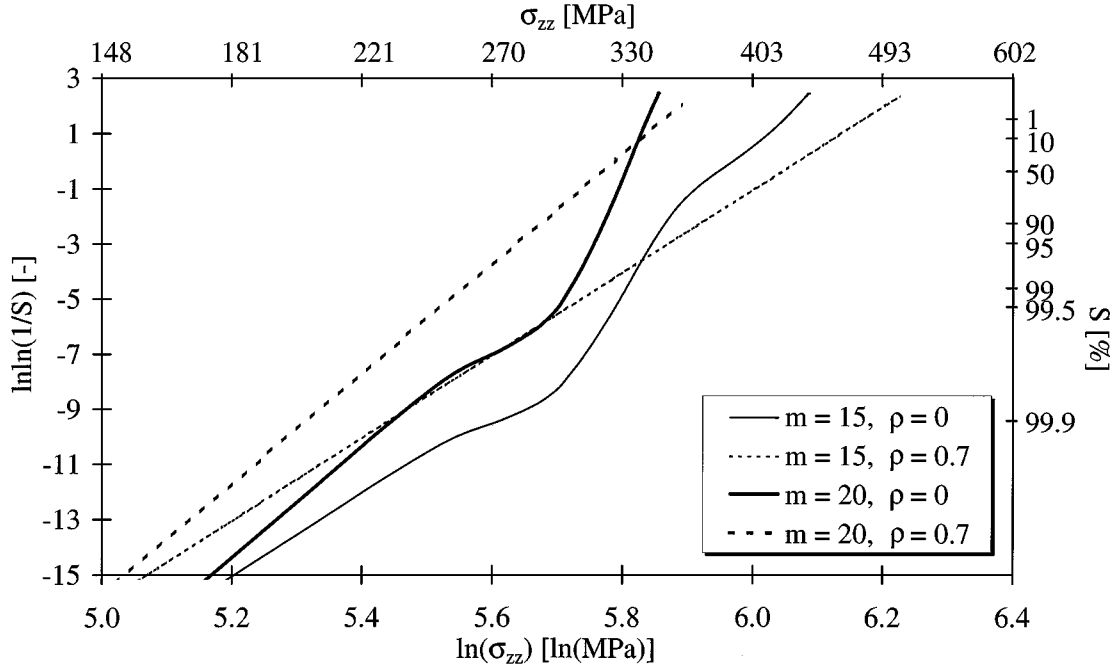

Figure 4 The survival probability S as a function of macroscopic axial stress σ_{zz} for $m = 15$ and 20 with loading ratios $\rho = 0$ and 0.7 (particle diameter $= 4\ \mu$m, $\sigma_{ys} = 276$ MPa, $n = 14.94$ and σ_0 350 MPa).

gradient 15, i.e. the survival probability variation of the unit cell equals that of the ceramic particle. However, when the stress exceeds $\ln(\sigma_{zz}) = 5.5 \approx 245$ MPa, some curvature occurs in case of $\rho = 0$, whereas the calculation with $\rho = 0.7$ remains a straight line. Furthermore, it is observed that a triaxial loading ratio results in a lower survival probability of the ceramic particle than the uniaxial loaded case.

From the above, it can be concluded that in case of $\rho = 0.7$, the survival probability of the ceramic particle is governed by a Weibull distribution, whereas for $\rho = 0$ this is no longer the case from the point where curvature starts.

5.2. Weibull modulus

To verify whether the gradient in Fig. 3 is the Weibull modulus m, calculations were also done for a different value ($m = 20$). The results of these calculations are shown in Fig. 4, where the survival probability is plotted as a function of macroscopic axial stress for $m = 15$ and 20, again with loading ratios $\rho = 0$ and 0.7 (particle diameter $= 4\ \mu$m, $n = 14.94$ and $\sigma_0 = 350$ MPa). These calculations result indeed in gradients 15 and 20, so the straight line indeed represents the Weibull modulus m. The overall appearance in case of $\rho = 0$ or 0.7 remains the same; i.e. a straight line of a gradient of the applied m for $\rho = 0.7$ and the occurrence of curvature for $\rho = 0$, whereby the shape of curvature differs slightly for both m-values.

5.3. Stresses in the particle

Equations 2 and 3 are valid for a uniform stress distribution in ceramics [11]. To investigate the uniformity of the stress inside the particle, 15 nodes near the interface were chosen and for these nodes the actual Drücker-Prager stress σ_{DP} was calculated with Equation 5 for both loading ratios $\rho = 0$ and 0.7 and plotted vs. the macroscopic axial stress σ_{zz} in Fig. 5.

It can be seen that there is a linear relation between σ_{DP} and σ_{zz} up to approximately 330 MPa in case of $\rho = 0$ and up to 1100 MPa in case of $\rho = 0.7$. When the stress becomes higher than 330 or 1100 MPa, σ_{DP} turns out to be dependent on the position in the particle, i.e. at the same macroscopic axial stress, all 15 nodes have a different Drücker-Prager stress. Because of the stress distribution in the particle not being uniform, the applied stress σ in Equations 2 and 3 should actually be replaced by $\sigma_{DP}(x) = \sigma_{zz} \cdot f(x)$ where $f(x)$ is some function of the position x in the particle. Equation 3 then becomes:

$$\ln\ln\frac{1}{S} = \ln\left(\frac{\int_v f(x)^m\, dV}{V_0}\right) + m \cdot \ln\sigma_{zz} - m \cdot \ln\sigma_0 \tag{7}$$

From this equation it can be seen, that as a result of non-uniformity of the stress, there is an additional factor, which explains the translation along the survival probability axis when going from $\rho = 0$ to 0.7.

To explain the curvature occurring for $\rho = 0$ in Figs 3 and 4, it can be concluded from Fig. 5 that, in a plot of $\ln\ln(1/S)$ vs. $\ln(\sigma_{zz})$, from the point where a straight line is no longer obtained, the stresses in the particle are not only non-uniform, but also non-proportional due to plasticity in the matrix surrounding the ceramic particle. Now, $f(x)$ in Equation 7 is also a function of σ_{zz}. For $\rho = 0$, it turns out that the regime where the stresses become non-proportional is just where the survival probability goes rapidly from 1 to 0, while for $\rho = 0.7$ this is at a stress of 1100 MPa, which will not be reached in this calculation. The latter can be seen in Fig. 6, in which the survival probability is plotted versus the macroscopic axial stress for the reference

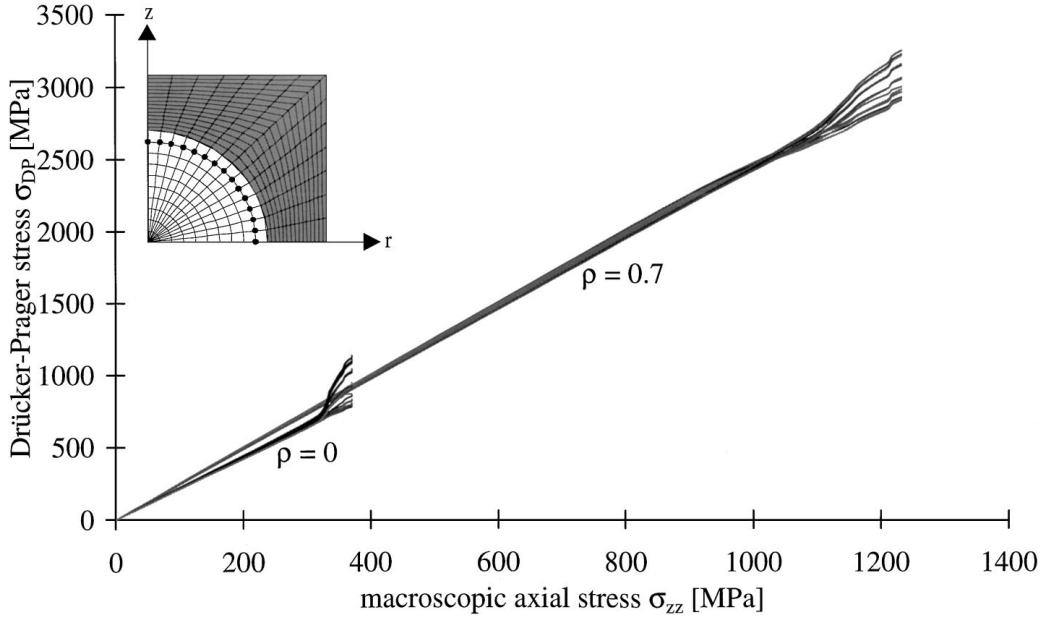

Figure 5 The Drücker-Prager stress σ_{DP} as a function of macroscopic axial stress σ_{zz} for 15 nodes near the interface of the particle with a diameter of 4 μm ($\sigma_{ys} = 276$ MPa and $n = 14.94$).

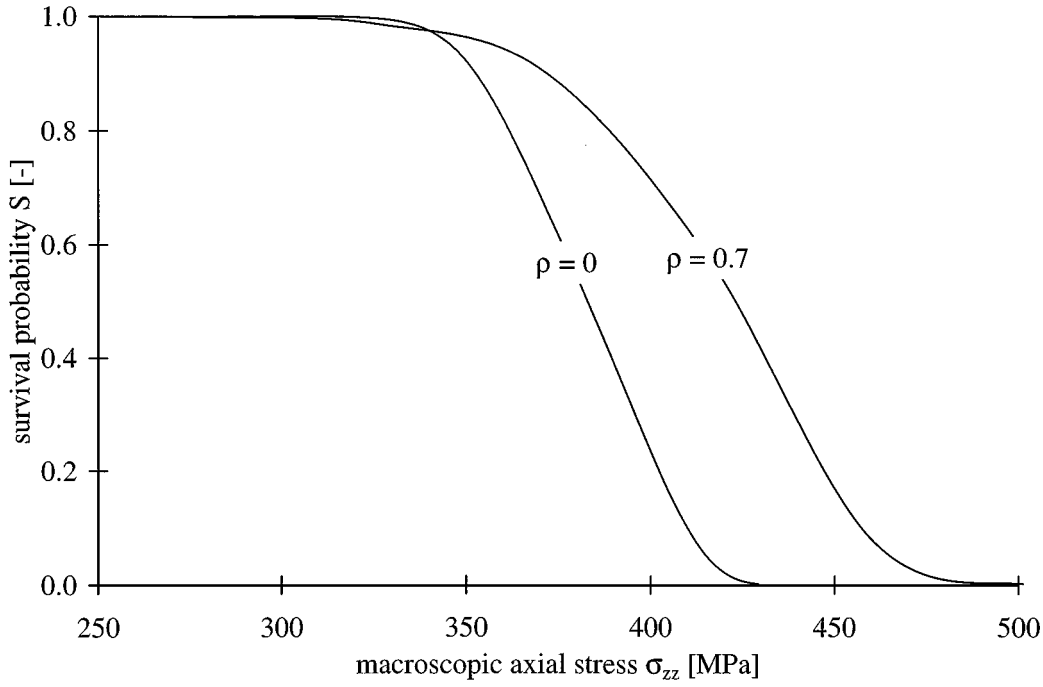

Figure 6 The survival probability S as a function of macroscopic axial stress σ_{zz} for a particle with a diameter of 4 μm, $\rho = 0$ and 0.7 ($m = 15$, $\sigma_0 = 350$ MPa, $\sigma_{ys} = 276$ MPa and $n = 14.94$).

configuration with $\rho = 0$ and 0.7, where for the latter a survival probability of zero is already reached at a macroscopic axial stress of 500 MPa.

5.4. Matrix hardening

If plasticity in the matrix surrounding the ceramic particle causes the curvature for $\rho = 0$, it seems useful to investigate the influence of different hardening exponents n for the aluminium matrix material. The results of these calculations are shown in Fig. 7. The survival probability is plotted as a function of macroscopic axial stress for an MMC with an AA 6061 matrix with hardening exponents $n = 4.35$ and 14.94 respectively, and loading ratios $\rho = 0$ and 0.7 (particle diameter = 4 μm, $m = 15$ and $\sigma_0 = 350$ MPa).

Again, a straight line of gradient 15 and the curvature in case of $\rho = 0$ above $\ln(\sigma_{zz}) = 5.5$ is observed. In case of $\rho = 0.7$, both calculations coincide completely and for $\rho = 0$ the calculations coincide up to the point where curvature starts. For $\rho = 0.7$, this means that a variation of the hardening exponent is of no influence since the matrix material remains elastic throughout the loading history. However, in case of $\rho = 0$, a lower hardening exponent results in less curvature; i.e. plasticity in the surrounding matrix occurs, but to a lesser extent as the hardening exponent becomes lower.

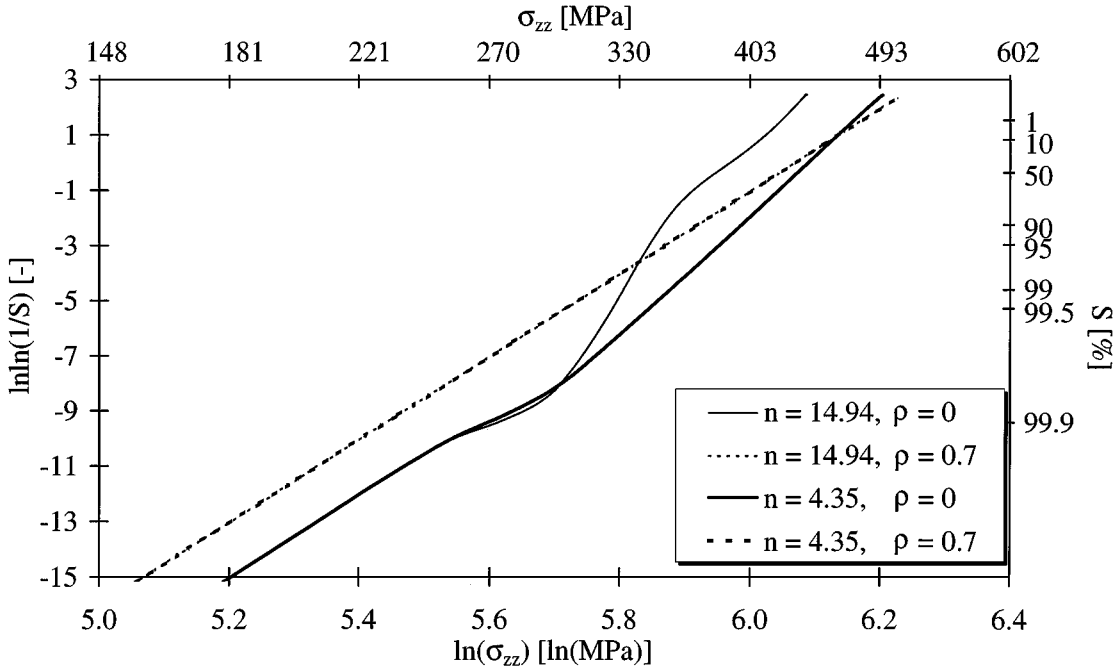

Figure 7 The survival probability S as a function of macroscopic axial stress σ_{zz} for hardening exponents $n = 4.35$ and 14.94 with loading ratios $\rho = 0$ and 0.7 (particle diameter = 4 μm, $m = 15$, $\sigma_{ys} = 276$ MPa and $\sigma_0 = 350$ MPa).

5.5. Characteristic stress and yield stress

When varying the characteristic stress σ_0, a parallel shift of the curves is observed. This can be seen in Fig. 8, in which for a particle with a diameter of 4 μm, $m = 15$ and $n = 14.94$, the results for characteristic stresses $\sigma_0 = 350$ and 525 MPa are shown for a loading ratio $\rho = 0$. As indicated in this figure, the shift between the calculations can be derived from Equation 7 as being $\ln(350/525)^{15} = -6.1$.

Since all calculations for $\rho = 0$ start with a straight line of gradient m, but start to curve when the macroscopic axial applied stress approximates the yield stress of the matrix material, results are also shown for calculations with three different matrix yield stresses namely, $\sigma_{ys} = 200$, 276 and 300 MPa. Equation 7 can be rewritten in the following equation:

$$\ln\ln\frac{1}{S} + m \cdot \ln\frac{\sigma_0}{\sigma_{ys}} = \ln\left(\frac{\int_v f(x)^m \, dV}{V_0}\right) + m \cdot \ln\frac{\sigma_{zz}}{\sigma_{ys}} \tag{8}$$

Now, if the left-hand term of this equation is plotted on the vertical axis and $m \cdot \ln(\sigma_{zz}/\sigma_{ys})$ on the horizontal axis, a 'mastercurve' can be created eliminating the effect of σ_0 and σ_{ys}. Two variables which still affect the mastercurve are the matrix hardening exponent and the Weibull modulus; the first changes the curvature and the latter results in a vertical shift. An example

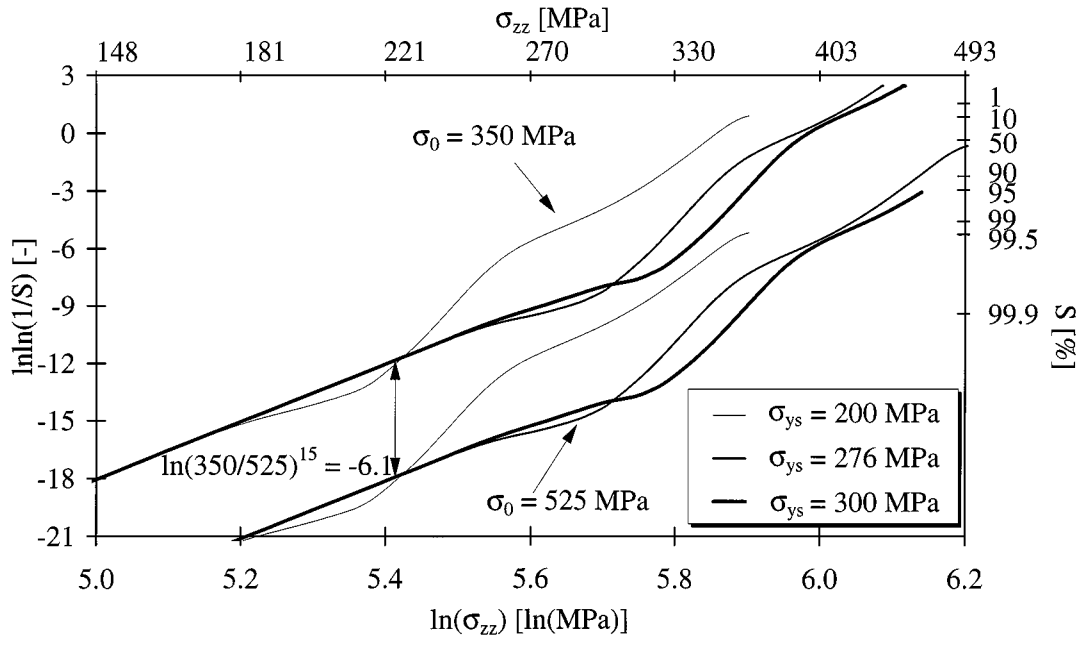

Figure 8 The survival probability S as a function of macroscopic axial stress σ_{zz} for characteristic stresses $\sigma_0 = 350$ and 525 MPa and matrix yield stresses $\sigma_{ys} = 200$, 276 and 300 MPa with loading ratio $\rho = 0$ (particle diameter = 4 μm, $m = 15$ and $n = 14.94$).

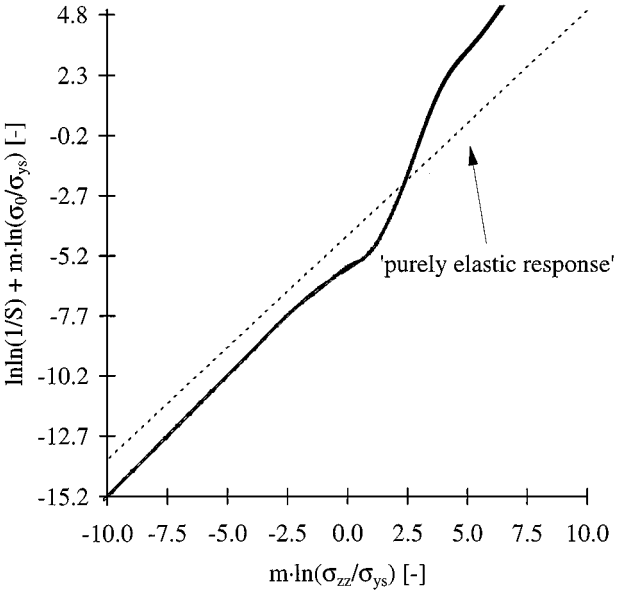

Figure 9 'Mastercurve' for characteristic stresses $\sigma_0 = 350$ and 525 MPa and matrix yield stresses $\sigma_{ys} = 200$, 276 and 300 MPa, all for a fixed value $n = 14.94$ and $m = 15$.

is given in Fig. 9 for $n = 14.94$. It turns out that, as long as all deformations in the MMC are purely elastic, $f(x)$ is independent on the applied stress, resulting in a gradient 1. As soon as plasticity in the surrounding matrix occurs, $f(x)$ becomes dependent on the applied stress and the mastercurve diverges from this gradient.

5.6. Particle size

Finally, when the particle diameter is doubled from 4 to 8 μm diameter, it can be seen in Fig. 10 that, for the same loading ratio, the survival probability decreases with increasing particle diameter. Besides a shift along the survival probability axis which can be explained with Equation 3 through the larger volume, the calculations for a particle with a diameter of 8 μm result in comparable lines as for a diameter of 4 μm; i.e. a straight line of gradient $m = 15$ in case of $\rho = 0.7$ and curvature above a certain σ_{zz}-value for $\rho = 0$. For 8 μm diameter it turns out that curvature is to a lesser extent than for 4 μm.

6. Conclusions

1. Based on present calculations it can be concluded that the relation between the macroscopic applied stress on the MMC and the survival probability of the ceramic particle can be described by the Weibull modulus m, as long as the stress distribution in the matrix surrounding the particle is proportional to the applied load, e.g. in Fig. 4, the particle should fail at a stress in the range where there is a linear relation between the Drücker-Prager stress σ_{DP} and the macroscopic axial stress σ_{zz}.

2. When loading the metal matrix composite triaxially ($\rho = 0.7$) instead of uniaxially ($\rho = 0$), the survival probability of the Al_2O_3 particle is lower and the particle is likely to fail before plasticity in the matrix occurs.

3. Considering the parameter dependence of particle fracture, it can be concluded that for the same loading ratio,

- an increase in the hardening exponent n of the matrix, results in coinciding calculations for $\rho = 0.7$ and 0; The calculations coincide up to the point where curvature starts, whereby a higher hardening exponent results in less curvature as a result of less plasticity in the matrix,
- a variation of the characteristic stress σ_0 results in a parallel shift of the curves for both $\rho = 0$ and 0.7,
- a 'mastercurve' for a fixed value of n can be made independent of characteristic stresses σ_0 and matrix yield stresses σ_{ys} and

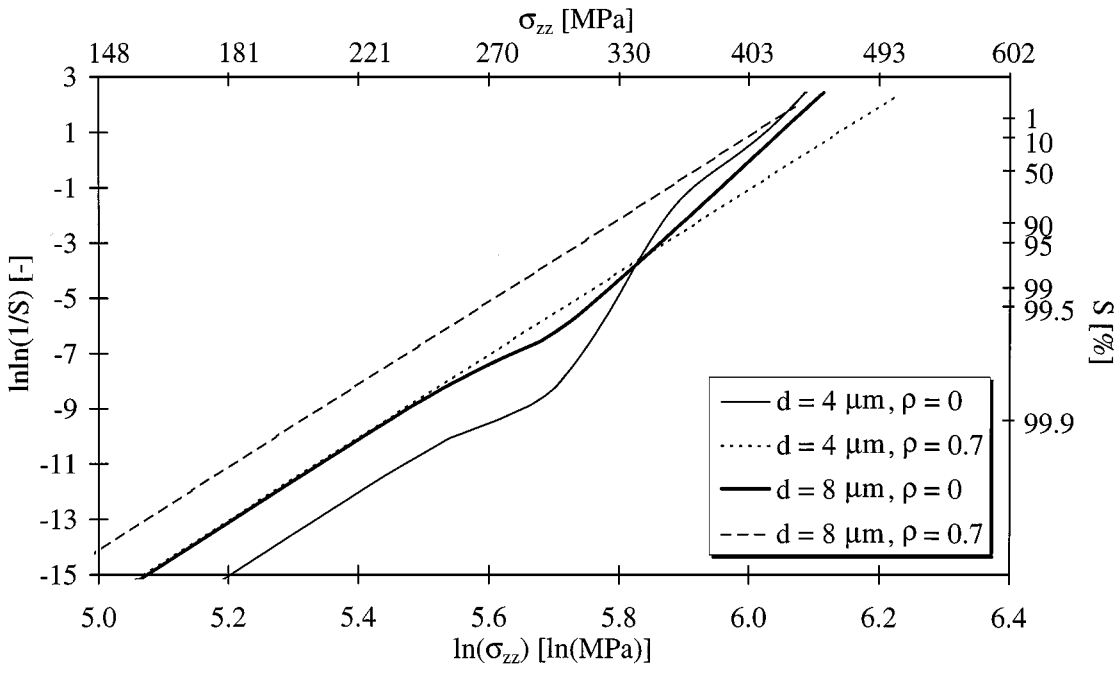

Figure 10 The survival probability S as a function of macroscopic axial stress σ_{zz} for particles with a diameter of 4 or 8 μm with loading ratios $\rho = 0$ and 0.7 ($m = 15$, $\sigma_0 = 350$ MPa, $\sigma_{ys} = 276$ MPa and $n = 14.94$).

- an increase of particle diameter (and thus volume of the ceramic particle) decreases the survival probability of an Al_2O_3 particle in an AA 6061 aluminium matrix.

References

1. T. W. CLYNE and P. J. WITHERS, in "An Introduction to Metal Matrix Composites" (Cambridge University Press, Cambridge, 1993).
2. C. A. LEWIS and P. J. WITHERS, *Acta Metall. Mater.* **43** (1995) 3685–3699.
3. Y. BRECHET, J. D. EMBURY, S. TAO and L. LUO, *ibid.* **39** (1991) 1781–1786.
4. T. MOCHIDA, M. TAYA and D. J. LLOYD, *Mater. Trans., JIM* **32** (1991) 931–942.
5. J. LLORCA, A. MARTÍN, J. RUIZ and M. ELICES, *Metall. Trans. A* **24A** (1993) 1575–1588.
6. D. J. LLOYD, *Acta Metall. Mater.* **39** (1991) 59–71.
7. J. KOPLIK and A. NEEDLEMAN, *Int. J. Solids Structures* **24** (1988) 835–853.
8. V. TVERGAARD, *Int. J. Fracture* **18** (1982) 237–252.
9. W. BROCKS, D. SUN and A. HÖNIG, *Comput, Mater. Sci.* **7** (1996) 235–241.
10. W. WEIBULL, *J. Appl. Mech.* **18** (1951) 293–297.
11. G. WEAVER, *J. Mater. Educ.* **5** (1983) 768–804.
12. C. A. LEWIS and P. J. WITHERS, *Acta Metall. Mater.* **43** (1995) 3685–3699.
13. J. LLORCA, *ibid.* **43** (1995) 181–192.
14. Metals Handbook, 9th ed., Vol. 8 (American Society for Metals, Metals Park, Ohio, 1985) p. 555.
15. MARC K7, MARC Analysis Research Corporation, Palo Alto, USA (1997).

Received 9 December 1998
and accepted 15 March 1999